

6. SYSTEM PERFORMANCE CALCULATIONS AND PREDICTIONS

System performance calculations can be made using the propagation models described previously in this paper. Antenna gains for the system performance predictions are factored in to represent the actual gains of these antennas. The final calculations take into account the antenna gains of the transmitter antenna at the transmitter site and the receiver antenna at the receiver site or test vehicle. In some systems analysis applications, it is necessary to calculate electric field strength near a receiver antenna knowing the received power level into a spectrum analyzer. When using a spectrum analyzer or receiver, correction must be made to the received power levels to calculate electric field strength in the vicinity of the receiver antenna, since most coverage calculations are in field strength.

The equation to calculate electric field strength, $E(\text{dBuV/m})$ from received power is [16]:

$$E(\text{dBuV/m}) = P_r(\text{dBm}) + 77.21 + 20 \log f(\text{MHz}) - G_r(\text{dBi}) + L_c(\text{dB}) \quad (65)$$

where $P_r(\text{dBm})$ is the received signal power which is referenced at the output of the antenna terminals but by appropriate adjustment of the losses can be moved to the reference point of the input to the spectrum analyzer or receiver, $f(\text{MHz})$ is the frequency in MHz, $G_r(\text{dBi})$ is the gain of the receiver antenna, and $L_c(\text{dB})$ is the loss in the cable.

The receiver antenna gain in this expression must also be corrected to account for the degradation in gain as a function of elevation angle for receiving a surface wave, sky wave, or space wave shown previously in Figure 4. The line-of-sight from the receiver to the transmitter antenna is typically at (depending on distance from the transmitter and receiver, and transmitter and receiver antenna heights above mean sea level) an elevation angle of less than a few degrees. Over this range of elevation angles the gain of the receiver antenna for a sky wave can vary from 10 to 20 dB or more below the main beam gain. The peak gain of this antenna is small due to the low antenna efficiency at these frequencies. This additional reduction in antenna gain due to elevation angle increases the electric field strength required for system operation, which is proportional to the decrease in antenna gain in decibels. This can be seen from equation (65) above.

The gain for launching and receiving a ground wave is calculated using the NEC code mentioned earlier and converting the computations in the output to an equivalent gain referenced to an isotropic radiator. The gain and pattern for launching and receiving a sky wave can also be computed using NEC directly, since it computes a space wave antenna pattern in addition to the specific information needed to obtain the ground-wave equivalent gain. The results of these calculations were shown in the previous section.

Once confidence is obtained in the prediction algorithms for antenna models, then predictions of area coverage of a station can be performed. Figures 18 and 19 show KTLK station coverage computed from the ITS model [7] for the daytime coverages for both smooth-Earth and smooth-Earth mixed-path propagation models. The differences in the two figures are a result of considering a mixed path.

The borders for the states of Colorado, Wyoming, and Nebraska are shown. Figures 20 and 21 show station coverage computed from the ITS model [7] for the nighttime coverages for both smooth-Earth and smooth-Earth mixed-path propagation models. The electric-field strength values are given in units of dB microvolts per meter (*dBuV/m*). They illustrate the difference in coverages when the mixed-path data are taken into consideration. The prediction with the smooth-Earth mixed-path model shows greater coverage near the station where the ground wave propagation predominates. The ground constants were taken from the data base contained in the LF/MF model [7]. The ground constants and the mixed path only affect the ground wave propagation, but station KTLK uses different antenna configurations for daytime and nighttime, which also affects antenna performance and coverage area. The transmitter power also changes from 1kW at night to 50 kW during the daytime. The nighttime antenna configuration was specifically designed to minimize the chance for interference at night to an adjacent or cochannel station northeast of station KTLK, because the sky wave makes it possible to propagate appreciable level signals at very long distances. The antenna array configurations for station KTLK were described in Table 2 previously. The patterns in these coverage plots are different than those in the actual antenna pattern predictions of Figures 14 and 15, because Figures 14 and 15 are equivalent gain antenna patterns for launching the surface wave described previously. Figures 20 and 21 were created by the model using a composite of the equivalent gain antenna patterns for the surface wave and the space wave antenna patterns for the skywave. The resulting combination will look different than the spatial gain distribution of the individual antenna patterns.

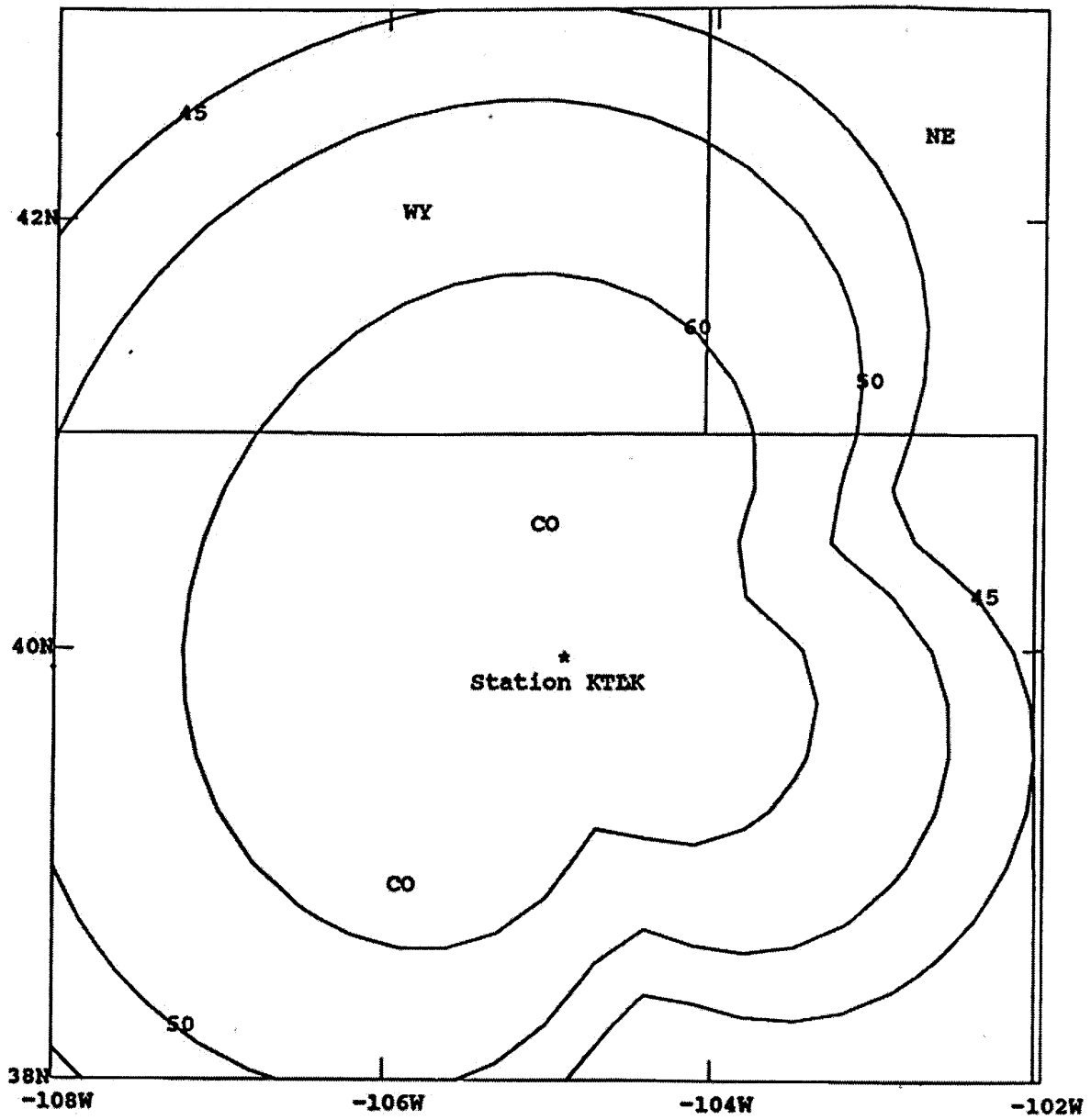


Figure 18. Predicted KTLK day coverage contours (dBuV/m) using the smooth-Earth model.

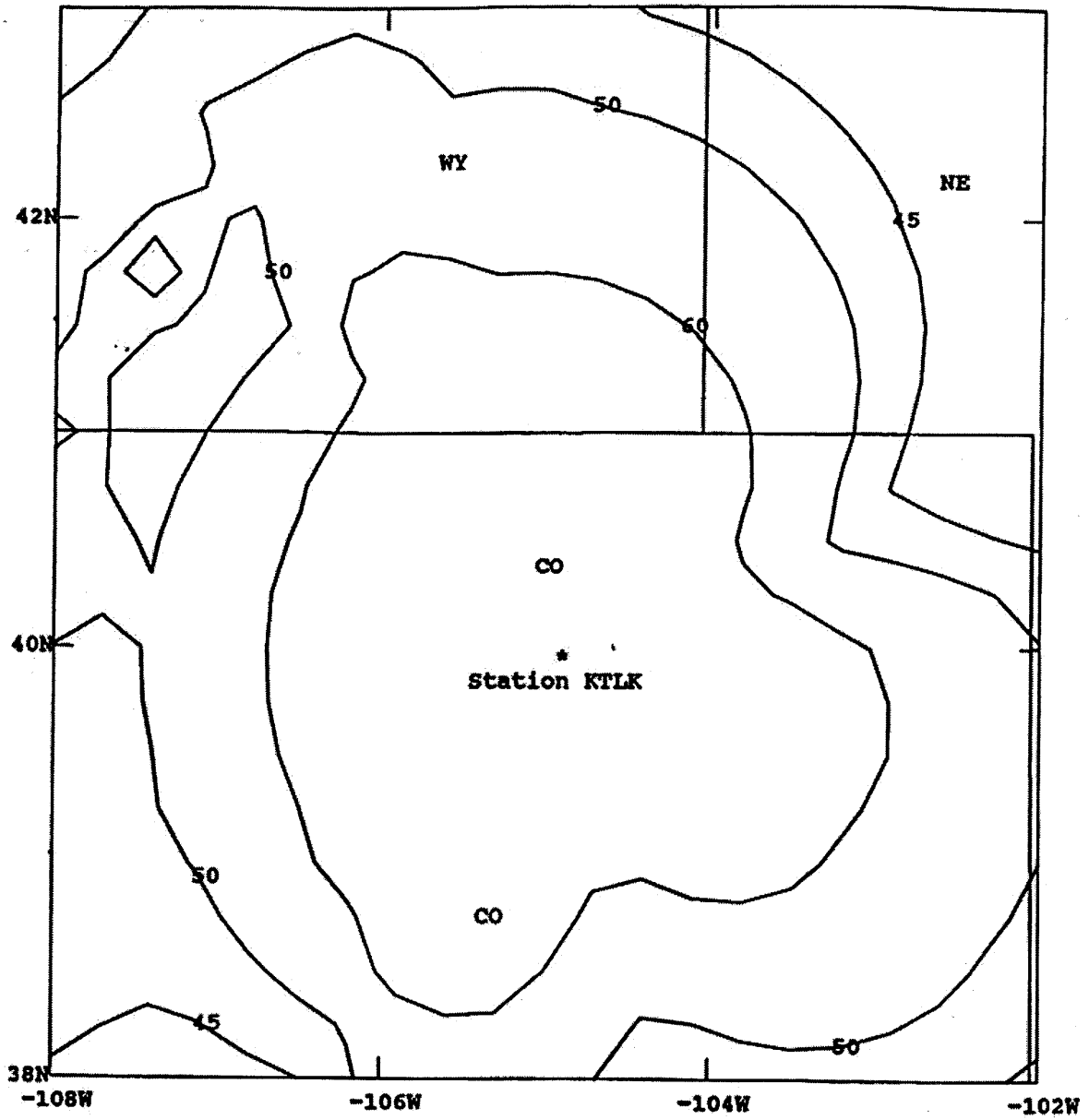


Figure 19. Predicted KTLK day coverage contours (dBuV/m) using the smooth-Earth mixed-path model.

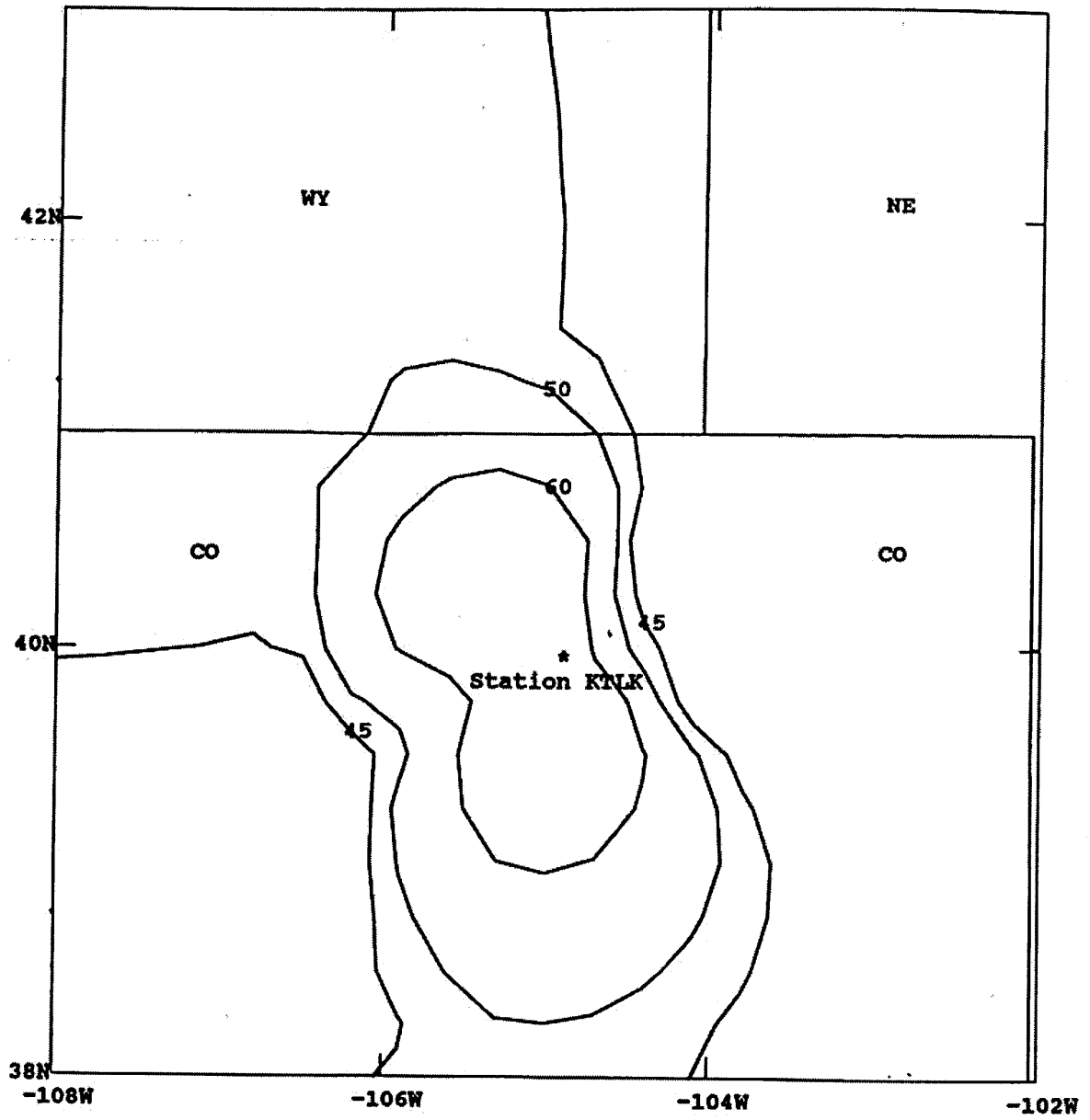


Figure 20. Predicted KTLK night coverage contours (dBuV/m) using the smooth-Earth model.

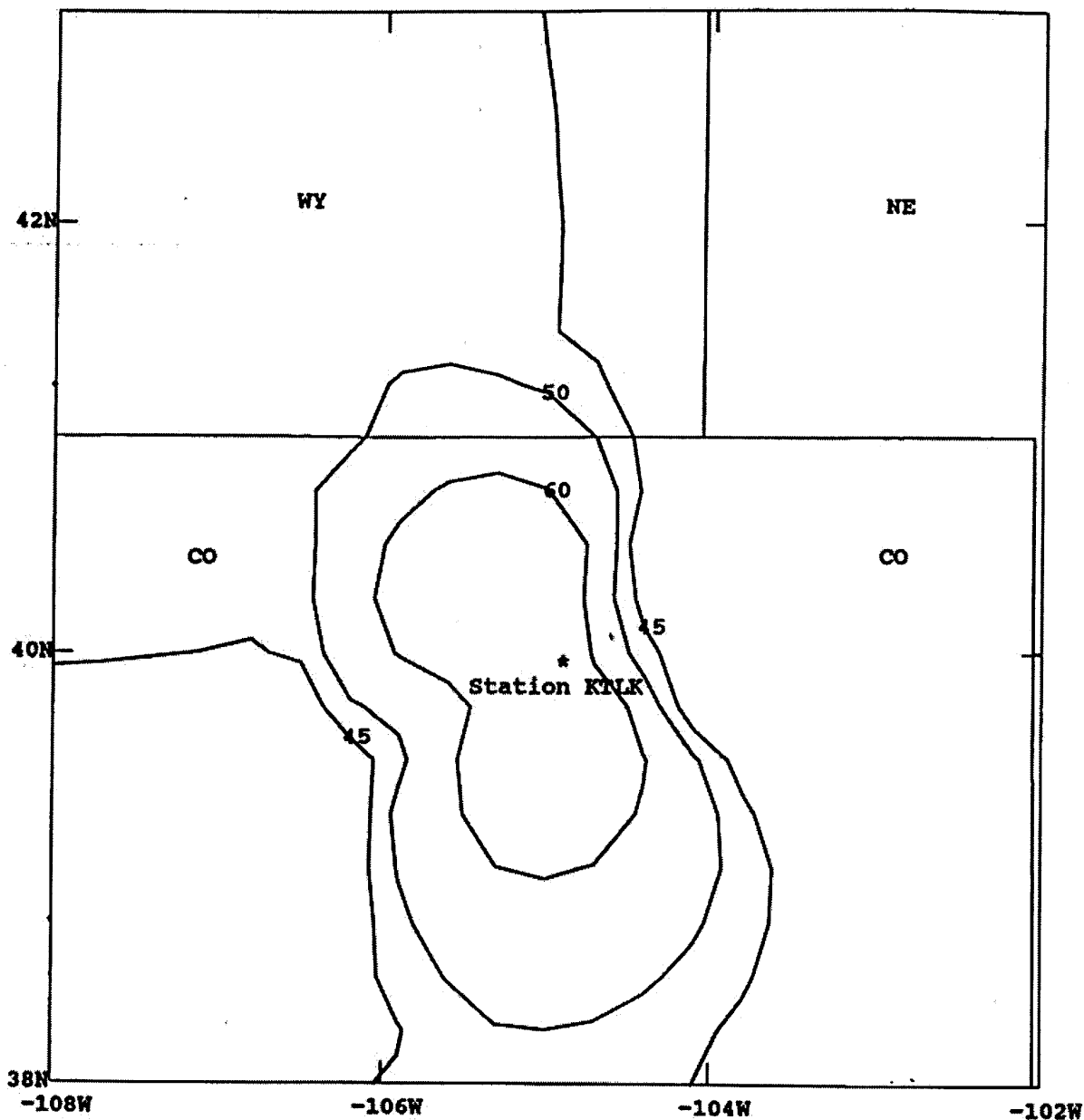


Figure 21. Predicted night coverage contours (dBuV/m) using the smooth-Earth mixed-path model.

The data used to plot Figures 22 and 23 were taken from the ITS model [7] using the point-to-point computation mode for the nighttime antenna configuration for the smooth-Earth and smooth-Earth mixed-path propagation models. Both figures are for a particular radial 330 degrees wrt due North for a long range nighttime prediction that includes both the ground-wave and the sky-wave components. The propagation model factors in the appropriate gains from the receiver and transmitter input geometry. The appropriate height-gain functions are also factored in to take into account nonzero antenna heights at both the transmitter and receiver locations. The combination of

the ground-wave and sky-wave propagation models also has an effect on the coverage, so the contours will look different than the spatial gain distribution of the antenna patterns. Both the ground wave and sky wave are plotted separately. When the sky-wave and ground-wave magnitudes become comparable to each other, they can combine constructively or destructively to either vectorially add together or produce a null at that particular distance from the station. The ground wave is a deterministic phenomenon, but the sky wave is a stochastic phenomenon, so the combination of the two is a stochastic process that will vary with time as ionospheric conditions vary. The smooth-Earth ground-wave model and the sky-wave model are equal at 170 km in Figure 22, but the smooth-Earth mixed-path ground-wave model in Figure 23 predicts that the ground wave and sky wave are equal at 190 km. The smooth-Earth mixed-path model is generally more accurate, since it takes into account the presence of a mixed-path ground constant condition if the data base of ground constants shows that it exists. The smooth-Earth model assumes a homogeneous Earth with one pair of values for the ground constants over the entire path.

System performance computations were made for several examples where measured data were available. Data were available from the DGPS site at Appleton [55,56]. Figure 24 compares the results of performance prediction calculations with the measured data for the Appleton, WA to Pendleton, WA path. The measured data for the Appleton site were obtained from reference [55]. The equivalent gain technique was used to determine antenna gains for system calibration. Figure 25 is a plot of the terrain contour over the Appleton to Pendleton path. The nulls of Figure 24 appear to correspond to when the measurement vehicle was located in deep canyons and behind large terrain peaks. Other extensive data were available for demonstrating agreement between predictions and measurements at various sites in the continental United States in the DGPS band of 285 to 325 kHz [56]. The reference [56] describes the results of comparisons of actual measurements to predictions over many paths. This DGPS signal is used for differential position correction of the GPS signal.

An extensive measurement program was performed at medium frequencies [40]. Figures 26 and 27 compare the measured data from two of the data runs at Canyonlands, Utah along a 45 km path from this reference with the model predictions. Data [40] were available from two medium frequency signals both at 520 kHz and 1618 kHz. There is good agreement between measurements and predictions. The irregular-Earth mixed-path model in the LF/MF model was used to perform the predictions, since the terrain is considered rough in comparison to a wavelength as shown in Figure 28. A smooth-Earth or smooth-Earth mixed-path prediction would not be accurate for this computation, since the terrain variations are large with respect to a wavelength. This reasoning was described earlier in the section on ground-wave propagation.

Propagation modeling and systems analysis can be used to resolve and explain actual measurements. An example of this can be demonstrated with recent measurements. A measurement was performed in Boulder, CO to determine the nighttime and daytime electric field strength received from the Appleton, WA DGPS site at 300 kHz (private communication J.R. Hoffman, February 8, 1999).

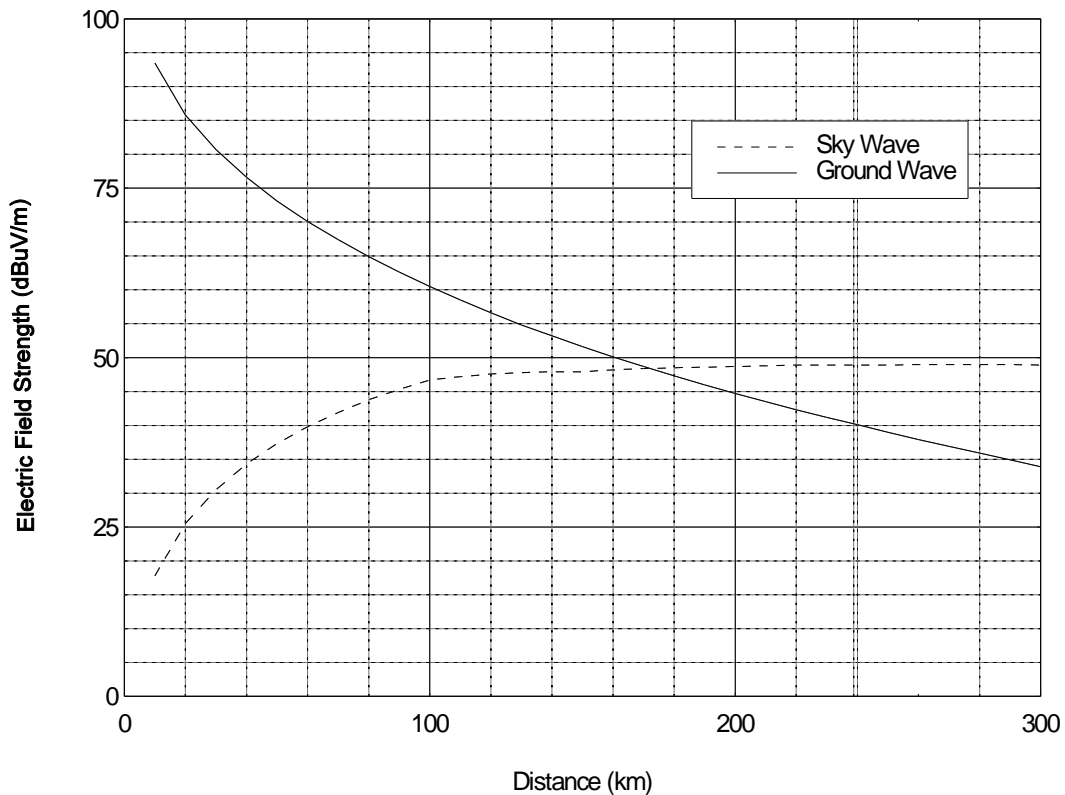


Figure 22. Electric field strength vs distance from station KTLK at nighttime on 330 degree radial using the smooth-Earth model.

Nighttime measurements of electric field strength consistently averaged 30 dBuV/m over several days with good quality DGPS messages. This is in good agreement with model predictions using the LF/MF model [7]. These results are shown in Figure 29 where contours of electric field strength from the Appleton DGPS site are plotted over a map of the Northwestern United States. Daytime measurements of 14 dBuV/m were also measured over several days, but there were no successful DGPS messages, since the signal levels from the Appleton DGPS site were too low. Predictions of electric field strength from the Appleton DGPS site resulted in -10 dBuV/m levels. This result is shown in Figure 30.

After searching a database of signals at this frequency, three other sites were found at 300 kHz. The LF/MF model was used to predict the daytime levels of electric-field strength from these sites. Two of these sites, one in Spearfish, SD and the other in Auburn, NE, were found to be capable of generating electric-field strengths at levels of 10 to 15 dBuV/m in the Boulder, CO area. Even though these two sites were at the same frequency, no successful DGPS messages were decoded since they were a different type of beacon site and were due to Federal Aviation Administration (FAA) beacons radiating at 300 kHz. The propagation model was able to account for the levels of electric field strength at 300 kHz in Boulder, CO that were measured.

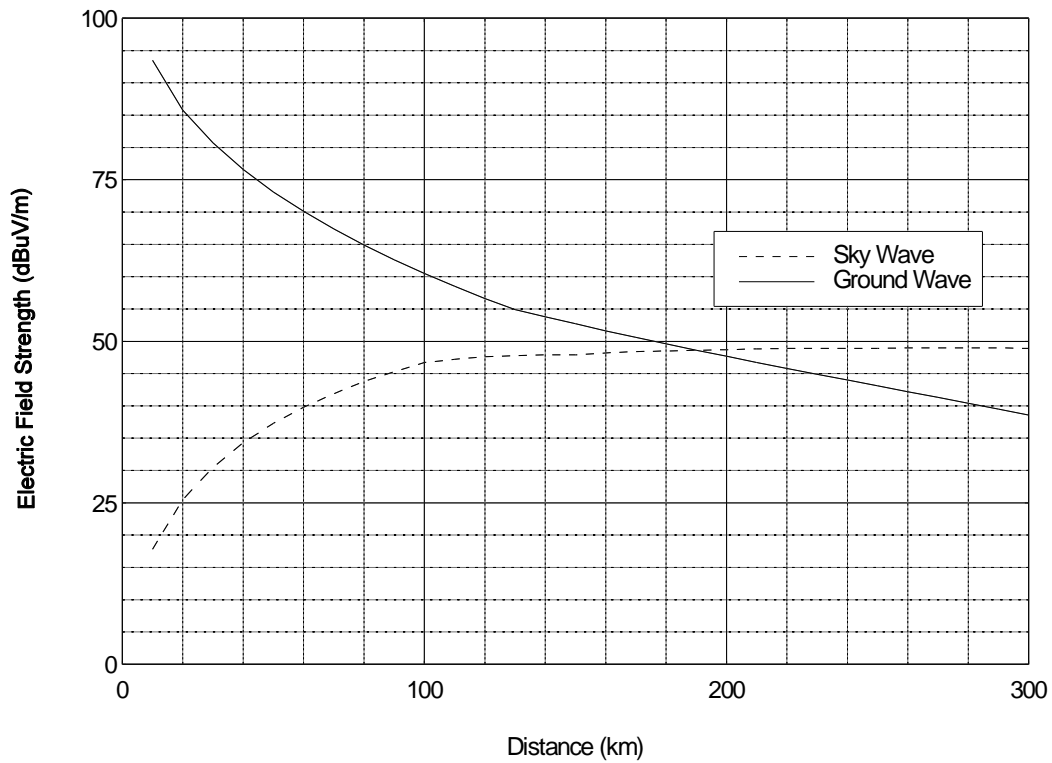


Figure 23. Electric field strength vs distance from station KTLK at nighttime on 330 degree radial using the smooth-Earth mixed-path model.

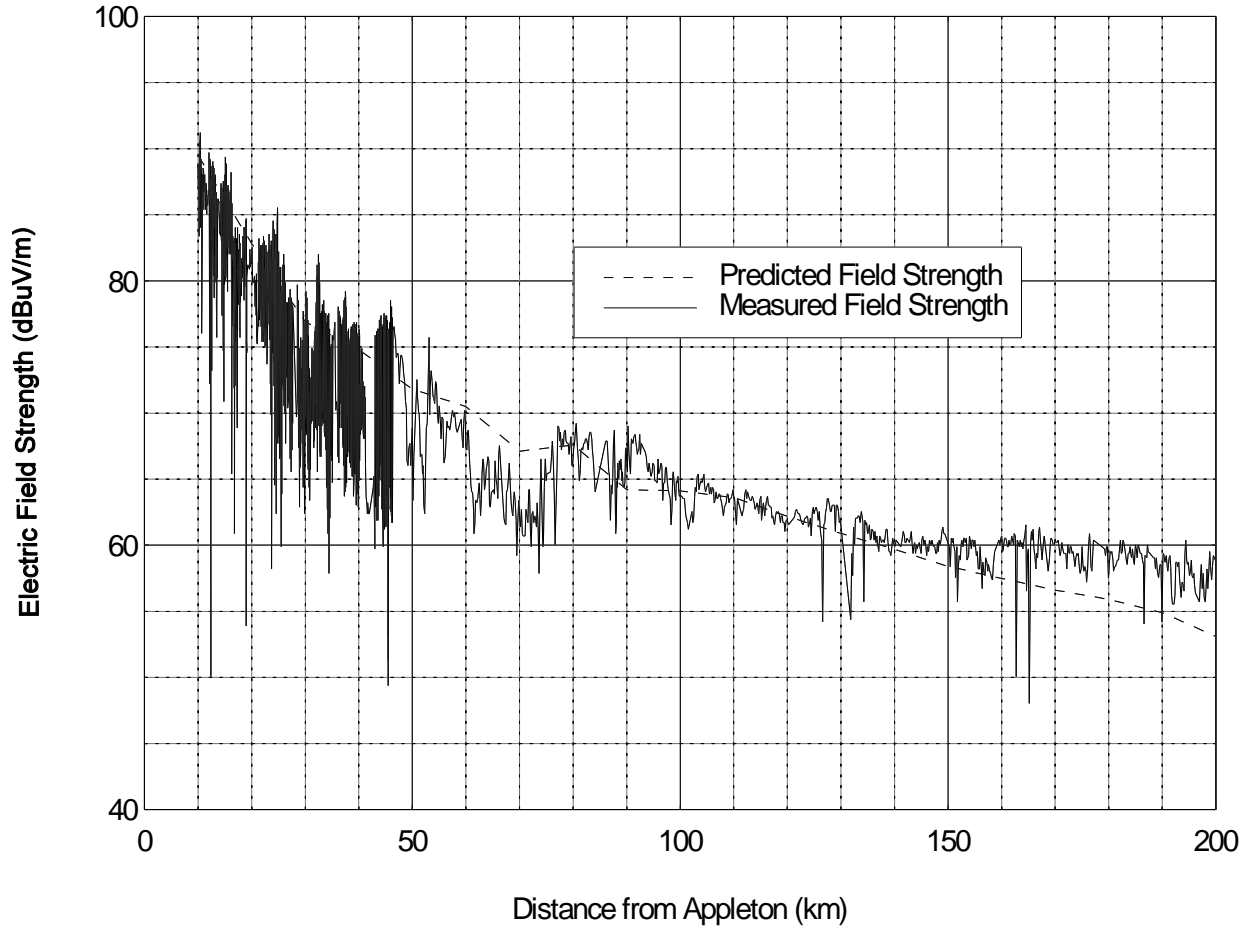


Figure 24. Comparison of measured and predicted DGPS field strength for the Appleton to Pendleton path.

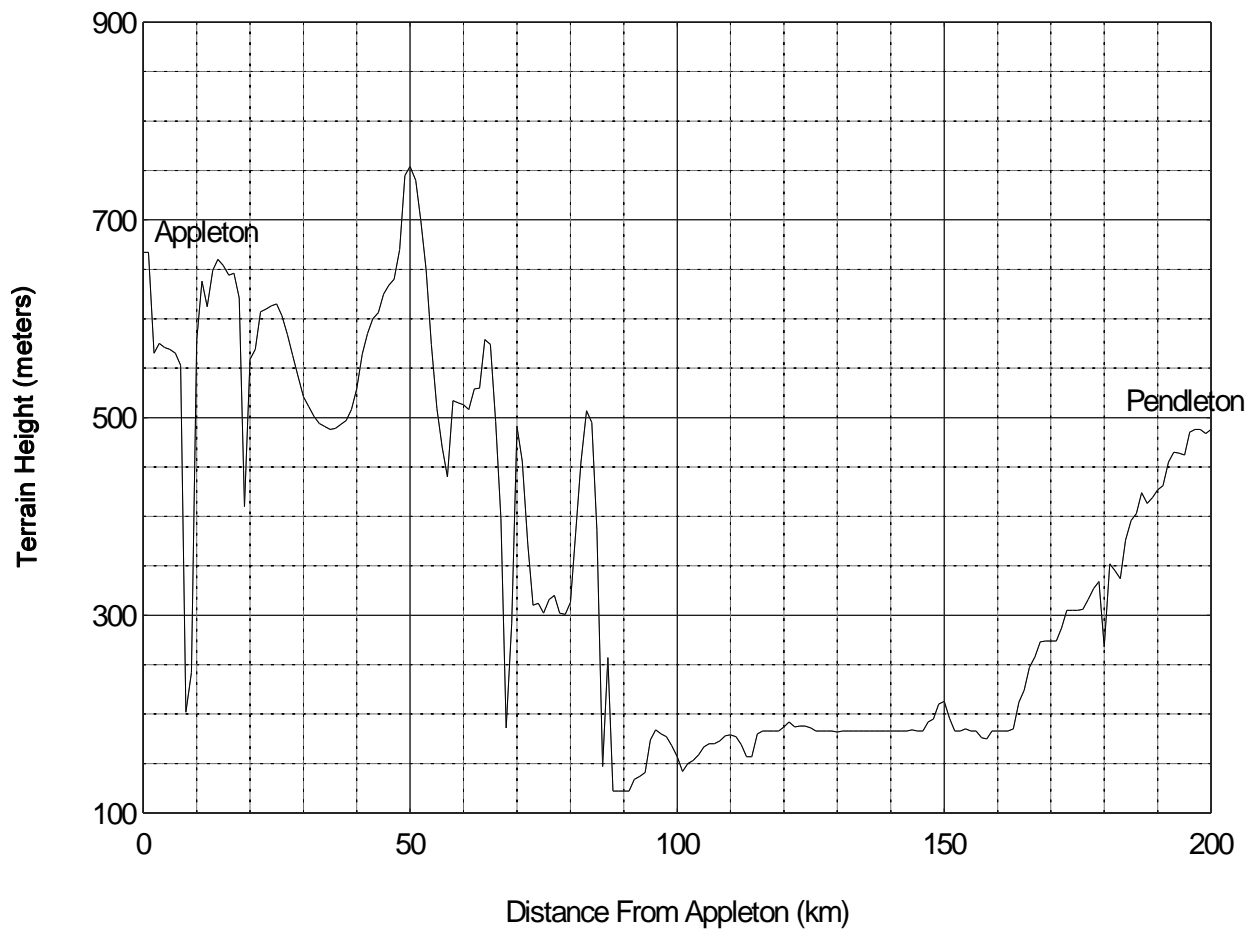


Figure 25. Terrain contour for path from Appleton to Pendleton, Washington.

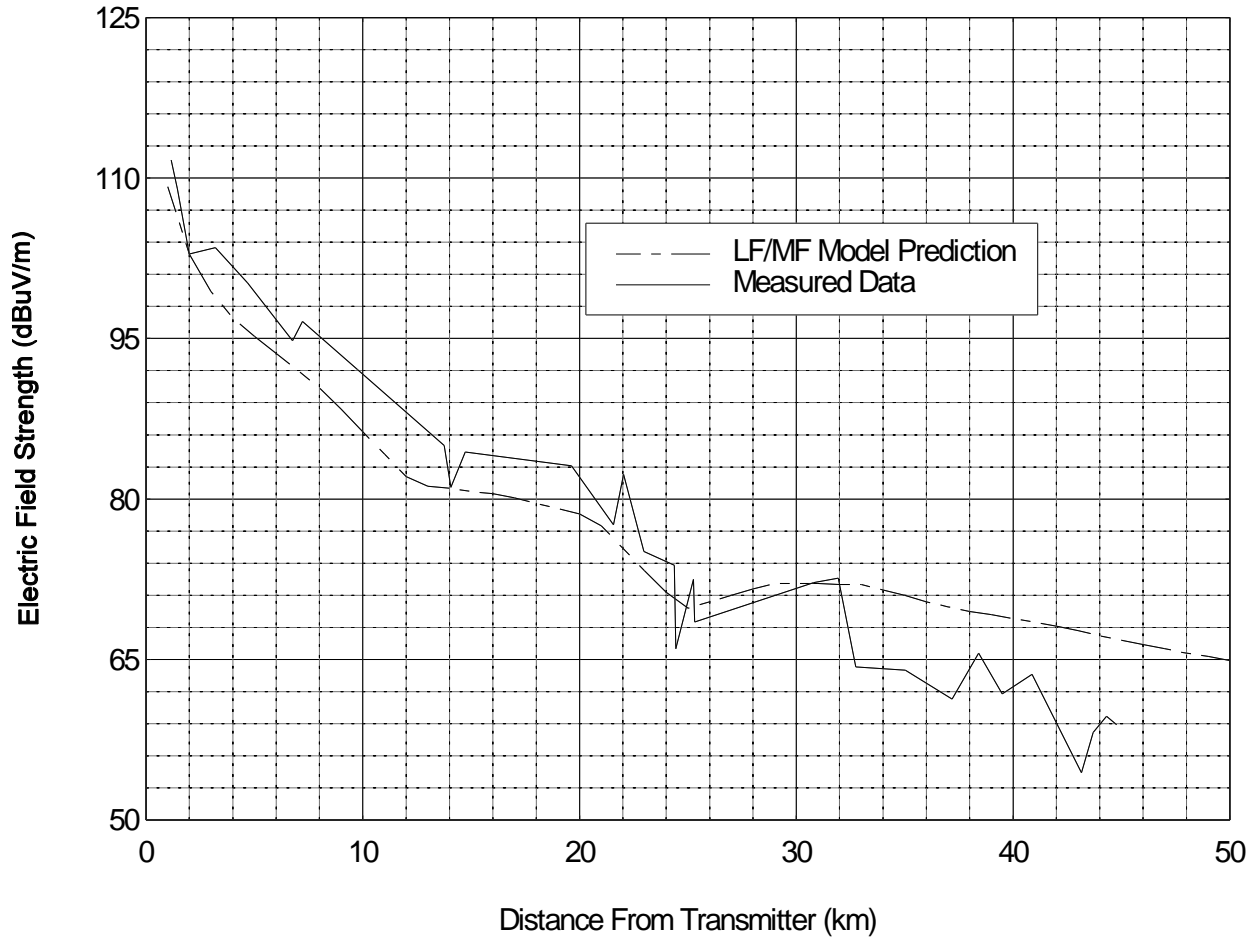


Figure 26. Comparison of measured and predicted data for Canyonlands, Utah path at 520 kHz.

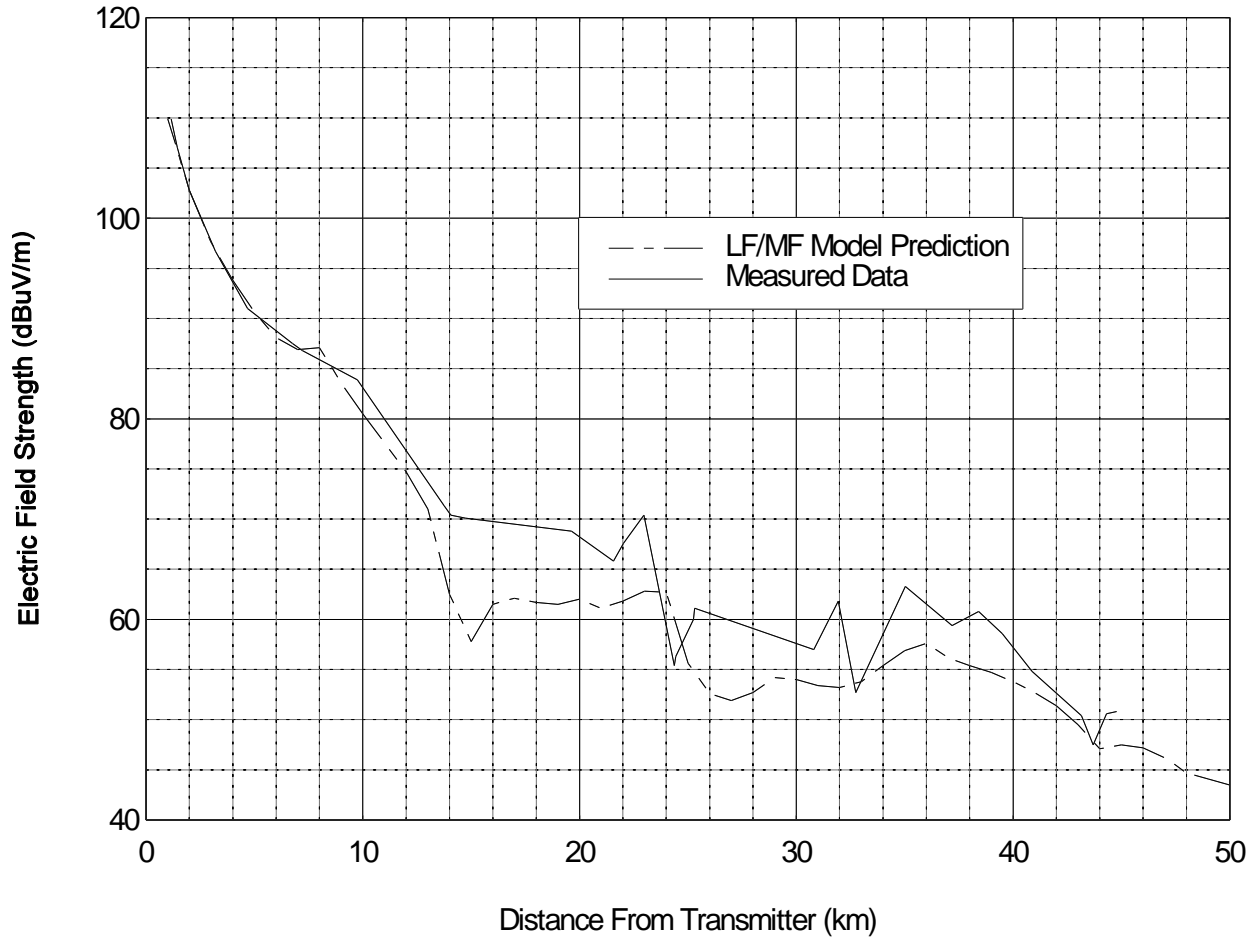


Figure 27. Comparison of measured and predicted data for Canyonlands, Utah path at 1618 kHz.

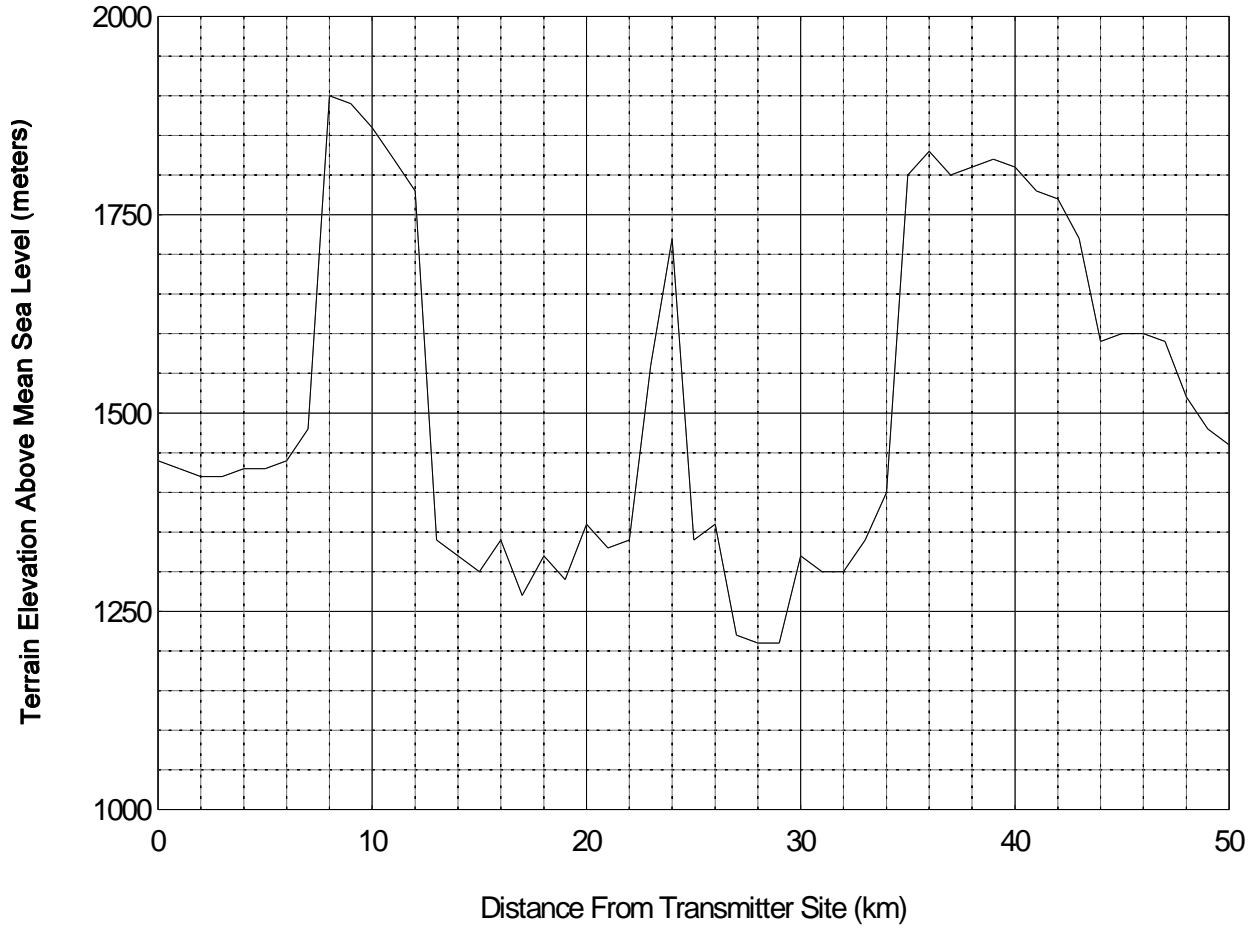


Figure 28. Terrain contour for Canyonlands, Utah measurement site.

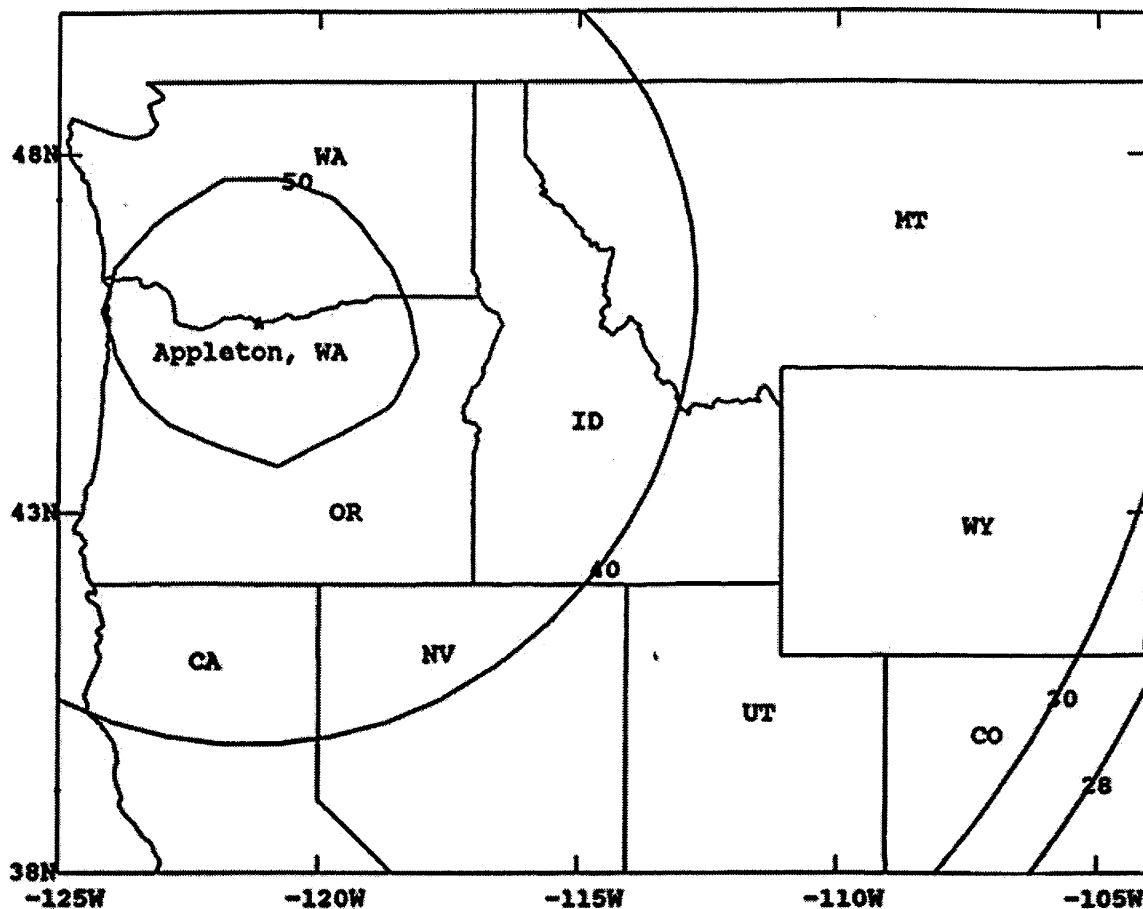


Figure 29. Contours of electric-field strength in dBuV/m from the Appleton, WA DGPS site at nighttime (f=300 kHz).

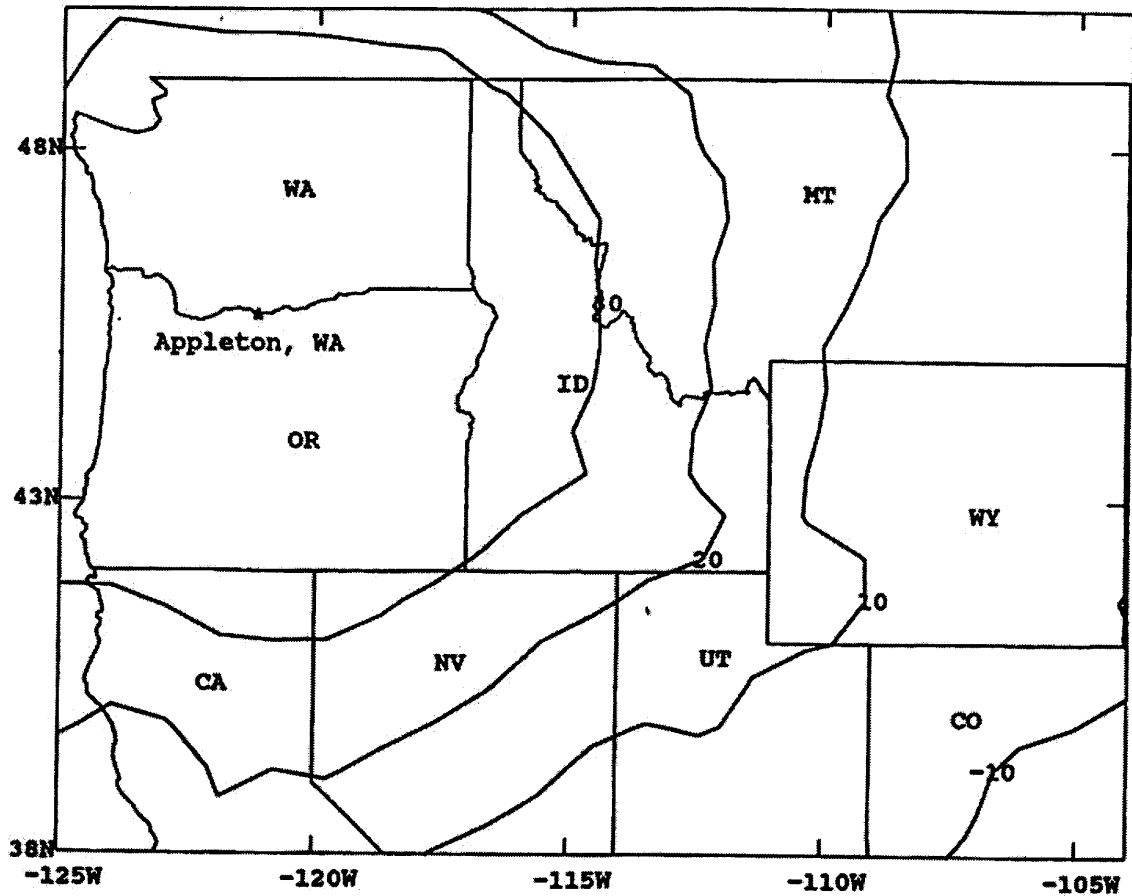


Figure 30. Contours of electric-field strength in dBuV/m from the Appleton, WA DGPS site at daytime ($f=300$ kHz).

7. CONCLUSION

This paper covered the basic aspects of radio-wave propagation and antenna modeling in the MF band. The MF band covers the frequencies of 300 to 3000 kHz. The sky wave models described in this paper are valid from 150 kHz to 1705 kHz. The ground wave models described in this paper are valid from 10 kHz to 30 MHz. In this paper the propagation models and antenna modeling techniques were shown to be quite different than those at other radio frequency bands. The propagation of radio waves in this band depends on both a ground wave and a sky wave and their interaction with the environment. The antennas are strongly influenced by the presence of ground and require numerical analysis techniques more sophisticated than free space techniques used in higher frequency bands. This paper describes radio wave propagation together with antenna